



Enhancing polyhydroxyalkanoate productivity with cell-retention membrane bioreactors

Burniol-Figols, Anna; Pinelo, Manuel; Skiadas, Ioannis V.; Gavala, Hariklia N.

Published in:
Biochemical Engineering Journal

Link to article, DOI:
[10.1016/j.bej.2020.107687](https://doi.org/10.1016/j.bej.2020.107687)

Publication date:
2020

Document Version
Peer reviewed version

[Link back to DTU Orbit](#)

Citation (APA):
Burniol-Figols, A., Pinelo, M., Skiadas, I. V., & Gavala, H. N. (2020). Enhancing polyhydroxyalkanoate productivity with cell-retention membrane bioreactors. *Biochemical Engineering Journal*, 161, Article 107687. <https://doi.org/10.1016/j.bej.2020.107687>

General rights

Copyright and moral rights for the publications made accessible in the public portal are retained by the authors and/or other copyright owners and it is a condition of accessing publications that users recognise and abide by the legal requirements associated with these rights.

- Users may download and print one copy of any publication from the public portal for the purpose of private study or research.
- You may not further distribute the material or use it for any profit-making activity or commercial gain
- You may freely distribute the URL identifying the publication in the public portal

If you believe that this document breaches copyright please contact us providing details, and we will remove access to the work immediately and investigate your claim.

1 Enhancing polyhydroxyalkanoate
2 productivity with cell-retention
3 membrane bioreactors
4

5 Anna Burniol-Figols, Manuel Pinelo, Ioannis V. Skiadas and Hariklia N. Gavala*

6
7 Technical University of Denmark (DTU), Dept. of Chemical and Biochemical Engineering,
8 Søltofts Plads, Building 228A, 2800 Kgs. Lyngby (Denmark)

9 *Corresponding author: hnga@kt.dtu.dk; hari_gavala@yahoo.com

10

11

12

13 Accepted manuscript. Biochemical Engineering Journal. <https://doi.org/10.1016/j.bej.2020.107687>

14

15 The article will undergo copyediting, typesetting, and review of the resulting proof before it is published in its final
16 form.

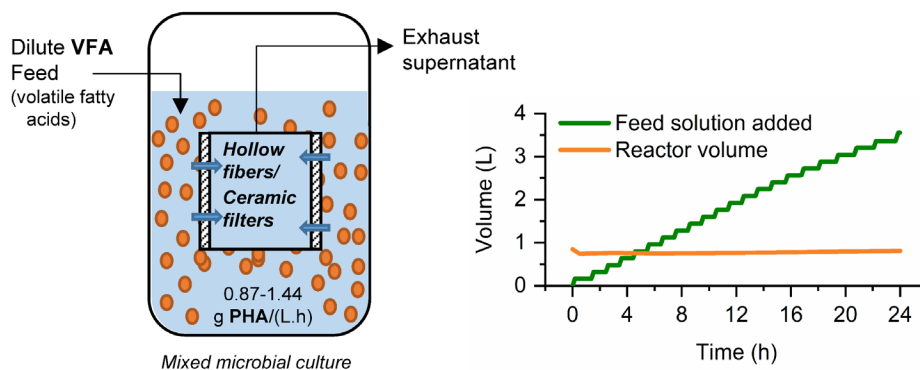
17 © 2020. This manuscript version is made available under the CC-BY-NC-ND 4.0 license

18 <http://creativecommons.org/licenses/by-nc-nd/4.0/>.

19 Abstract

20 One of the factors limiting the economic viability of polyhydroxyalkanoates (PHA) is the low volumetric
21 productivity obtained with second-generation feedstocks, resulting from their low carbon concentration.
22 In the present study, the use of membrane bioreactors (MBRs) was evaluated as a strategy to retain the
23 microbial cells in the reactor and to enable a repeated supply of substrate without increasing the reactor
24 volume. Two immersed MBR systems were studied: classical pressure-driven MBRs (hollow fibers and
25 ceramic filters), and a novel diffusion-based MBR. In the latter, the rate of volatile fatty acid (VFA)
26 diffusion across the membranes was lower than the VFA consumption rate of the culture, and thus, not
27 suitable to attain high productivities. Possible research directions to increase substrate diffusion are
28 suggested. On the other hand, pressure-driven configurations led to high values of productivity (0.87-1.44
29 g PHA/(L.h)) during a fed-batch PHA accumulation using mixed microbial consortia. No flux reduction
30 was observed in a 24 h fed-batch process, which allowed for a reduction of up to 82 % of the reactor
31 volume, demonstrating the potential of this strategy. Hollow fibers and ceramic filters offered similar
32 results during the fed-batch, but they presented different limitations and advantages.

34 Graphical abstract



35

36 1 Introduction

37 The interest in biodegradable and biobased plastics has increased intensely during the last decades, due to
38 their potential to mitigate some of the environmental impacts caused by petroleum-derived plastics.

39 Among them, polyhydroxyalkanoates (PHA) have received significant attention given their high
40 biodegradability, wide range of applications, and possible raw materials [1]. Yet, PHA represent only a
41 minor percentage of the bioplastics market, which is to a big extend, due to their high production costs
42 [1].

43 Microbial cultivation techniques allowing for high values of PHA productivity (frequently in the range of
44 2-3 g PHA/(L.h)) were already reported during the 90s [2,3]. These strategies implied the use of axenic
45 cultures, highly purified and concentrated feedstocks, and pure O₂ supply. All of which are factors that
46 translate into high operational costs. Over the years, the focus has shifted to organic waste streams which,
47 besides reducing costs, would bring improvements in terms of sustainability [1,2,4]. For similar reasons,
48 the use of mixed microbial consortia (MMC) is emerging, owing to their low operational demands [1,5].

49 Values of volumetric PHA productivity obtained with second-generation feedstocks have rarely surpassed
50 values of 1 g PHA/(L.h), neither in pure cultures or MMC [2,4,5]. Hence, there is a need for developing
51 efficient cultivation techniques to produce PHA from these substrates. One of the main challenges is the
52 low carbon concentration in such feedstocks, which causes volume increase during fed-batch cultivations
53 [1,3,4]. A way to circumvent this issue is the use of membrane bioreactors (MBRs) with cell-retention
54 systems, which enable removal and addition of feed while keeping the cells in the bioreactor.

55 MBRs have been extensively applied in wastewater treatment [6] and increasingly in other
56 biotechnological applications [7], but little research has been performed on the frame of PHA production.

57 A few studies have explored the use of external loop MBRs in PHA production bioreactors with pure
58 cultures [8–11]. In such systems, the fermentation broth is recirculated through an external cross-flow
59 filtration module, where part of the supernatant is removed (Figure 1). High PHA productivities were

60 reported, up to 4.6 g PHA/(L.h) in Ahn et al.[8]. However, external loop MBRs rely on high cross-flow
61 velocities to control membrane fouling, which result in high operational costs [6,12]. Moreover, cell
62 recirculation can lead to shear stress or oxygen limitation, resulting in cell death or reduced cell growth
63 [6,7,13].

64 Operational costs are generally lower in immersed MBR configurations (iMBR), in which the filtration
65 modules are submerged in the cell broth and aeration can provide fouling control [7,12] (Figure 1). To the
66 extent of our knowledge, iMBRs have only been tested for PHA production in the study of Kumar et al.
67 [14], resulting in a two-fold increase in the cell concentration. Yet, the productivity of the system was low
68 (< 0.1 g PHA/(L.h)) due to the low PHA yield of the strain.

69 Both immersed and external loop MBRs are based on the application of a pressure differential as the
70 driving force to achieve liquid permeation across a membrane (commonly by applying suction on the
71 permeate side) [6,15] (Figure 1). More recently, an alternative MBR strategy has been suggested, using
72 concentration gradients as the driving force [6,15] (Figure 1). In such systems, the microorganisms are
73 separated from the feed medium by means of a membrane, which allows diffusion of the substrate to the
74 cell compartment due to the difference of concentration. Experience on these systems is very limited, and
75 so far only focused on anaerobic processes [15]. Membrane fouling - the main challenge of MBRs - can
76 still occur, but it is less likely, as the magnitude of the force bringing the cells and other foulants to the
77 surface of the membrane is smaller.

78 In the present study, immersed pressure-driven and diffusion-based MBR configurations were tested for
79 the first time in the frame of PHA production using MMC. The main objective was to provide a proof of
80 concept of their utilisation to overcome the volume limitations imposed by diluted feed solutions. Despite
81 they are both immersed systems, the abbreviation iMBR is kept for conventional immersed pressure-
82 driven MBRs, while dMBR is used to refer to diffusion-based MBR configurations.

83 2 Materials and methods

84 2.1 PHA-producing culture

85 PHA producing culture was enriched and maintained in a Sequential Batch Reactor (SBR) of 1.7 L
86 working volume, run under aerobic feast-famine regime as described in [16]. Briefly, the reactor followed
87 a cyclic operation, where every 12 h, half of the volume of the reactor (850 mL) was replaced with fresh
88 medium containing crude glycerol, butyrate, propionate, and acetate, to a substrate concentration of 45
89 C_{mM} at the beginning of each cycle. The effluent at the end the cycle was used as inoculum for the PHA
90 accumulation without any prior sedimentation. The culture was dominated by the genera *Thauera* and
91 *Ammaricoccus* [16].

92 2.2 Feed solution

93 The feed for the PHA accumulation was a synthetic mixture of VFA, simulating the concentration of
94 VFA obtained experimentally after optimisation of crude glycerol fermentation in continuous mode
95 (operated at pH 6.4, HRT of 10 h and 50 g/L of glycerol) [17]. The fermentation effluent contained
96 butyrate (6.4 g/L), propionate (1.8 g/L), acetate (1.1 g/L) and lactate (0.75 g/L). Soluble ammoniacal
97 nitrogen ($N-NH_3$) and phosphate (PO_4^{3-}) were 10.8 and 501 mg/L, respectively, corresponding to a
98 nitrogen/carbon ratio (N/C) of 1.8 N_{mmol}/C_{mol} , and a phosphorous/carbon ratio (P/C) of 11.9 P_{mmol}/C_{mol} .
99 For the experiments described in section 2.3 (effect of N/C ratio) and due to volume limitations (see
100 below), the VFA concentration was 10 times higher than in the model effluent. The proportion of each
101 VFA and the P/C ratio was the same as in the model effluent. Different N/C ratios were tested (explained
102 in section 2.3). For the experiments described in section 2.4 and 2.7, the VFA concentration and the P/C
103 ratio was the same as in the model effluent and the N/C ratio was adjusted to 15 N_{mmol}/C_{mol} .

104 For all experiments, the VFA solution was prepared in BA Medium [17] and adjusted to pH 6.4 with
105 NaOH. N/C and P/C ratios were adjusted with NH_4Cl and K_2HPO_4 . Antifoam 204 (Sigma Aldrich) and
106 allylthiourea were added to a final concentration of $85 \mu\text{L/L}$ and 5 mg/L .

107 **2.3 Fed-batch PHA accumulation: effect of the nitrogen/carbon ratio**

108 PHA accumulation experiments were performed in a Multifors reactor (1.4 L) (Infors HT, Switzerland)
109 with a starting volume of 650 mL of inoculum. The culture was fed with a VFA medium (section 2.2), in
110 which the VFA concentration was 10 times higher than in the model effluent to circumvent the volume
111 limitation of the reactors. Four experiments were performed at different N/C ratios ($N_{\text{mmol}}/C_{\text{mol}}$): 1.8 (as in
112 the model effluent), 15, 30 and 50. The experiments with N/C ratios of 1.8 and 15 ran simultaneously in
113 parallel reactors using inoculum from the same SBR cycle. The experiments at N/C ratios of 30 and 50
114 also ran simultaneously on another SBR cycle.

115 Experiments were performed in fed-batch mode for 24 h. Medium was initially added to a VFA
116 concentration of $90 C_{\text{mM}}$ (14 mL of medium). Thereafter, the same feeding volume was repeated
117 whenever butyrate was exhausted, manifested by an increase of more than 8 % in the dissolved oxygen
118 saturation ($p\text{O}_2$) with respect to the $p\text{O}_2$ immediately after substrate addition. Aeration, agitation,
119 temperature and pH were kept at 1 L/min, 750 rpm, $30 \text{ }^\circ\text{C}$ and pH 8, respectively.

120 **2.4 Diffusion-based MBR configuration (dMBR)**

121 VFA diffusion was tested in two membrane materials: PSf (polysulfone) and PVDF (poly(vinylidene
122 fluoride)), both with a poly(propylene) support layer. The PSf membrane had a pore size of $0.2 \mu\text{m}$
123 (GRM0.2PP, Alfa Laval, Sweden – $270 \mu\text{m}$ thickness). Two pore sizes (0.15 and $0.45 \mu\text{m}$) were tested
124 for the PVDF membrane (FSM0.15PP and FSM0.45PP, Alfa Laval, Sweden - $285 \mu\text{m}$ thickness). Before
125 use, the membranes were cleaned with distilled water (dH_2O) and dilute NaOH (pH 10) at $45 \text{ }^\circ\text{C}$
126 according to the manufacturer instructions.

127 The membranes were placed in an aluminium support inside the bioreactor, separating the bioreactor in
128 two concentric compartments (Figure 2). The internal compartment contained the microbial culture.
129 Aeration (1 L/min), agitation (750 rpm) and pH control (pH 8) were performed in this compartment. The
130 feed was supplied in the external compartment, which was cell free. The membranes were placed with the
131 active membrane surface in contact with the external compartment. The total active surface of the
132 membrane was 312 cm².

133 To test VFA diffusion across the membranes, the external compartment was filled with 160 mL of
134 medium at pH 6.4 (section 2.2). The internal compartment was loaded with 650 mL of autoclaved
135 inoculum (to avoid VFA consumption). The VFA diffusion rate (in C_{mmols/h}) was calculated from the
136 slope of the VFA amount detected in the inner compartment vs. time during the first 30 min, and thus
137 corresponded to the initial and maximum VFA diffusion rate.

138 **2.5 Immersed pressure-driven MBR configurations (iMBR)**

139 **2.5.1 Hollow fibers**

140 Hollow fiber modules were purchased from Zena Membranes (Czech Republic). They consisted of
141 poly(propylene) fibers with an average pore size of 0.1 μm and an external and internal diameter of 310
142 and 240 μm, respectively. Two types of membrane configurations were tested: a rod configuration
143 (Figure 3 A) and a loop configuration (Figure 3 B). The rod consisted of 800 fibers of 10 cm length, and
144 the loop was made of 400 fibers of 20 cm. Both configurations had a filtration surface of 779 cm² and
145 were connected to a poly(vinyl chloride) (PVC) pipe placed in a 12 mm port in the bioreactor. In order to
146 minimise the internal volume of the PVC pipe, a tube of 2 mm diameter was placed inside, directly
147 connecting the outlet of the pipe to base of the pipe. For the loop configuration, a plastic net was fixed
148 between the agitation shaft and the filter module to avoid damage by the impellers (Figure 3 B).

149 Before the first use, the fibers were soaked in 2-propanol for 30 min and rinsed with dH₂O. The fibers
150 were always kept in dH₂O to prevent drying. In between experiments, the fibers were cleaned with NaOH

151 0.1 wt%, citric acid 2 wt% and dH₂O. For each reagent, the cleaning consisted of three steps: soaking,
152 filtering and backflushing (30 min each). dH₂O permeability was measured before each experiment.

153 **2.5.2 Ceramic filters**

154 The ceramic filtration module was built with 8 ceramic cylinders (silicone carbide) of 10 mm external
155 diameter, 6 mm internal diameter and 12 cm length (LiqTech International, Denmark). The active
156 filtration layer was on the external part of the cylinders (0.5 µm pore size) (Figure 4). The filters were fit
157 in a stainless steel support secured with threaded rods and sealed with silicone. The upper part of the
158 support connected the internal volume of all filters to a single steel outlet tube fixed to one of the ports of
159 the bioreactor. The active surface area of the module was 276 cm². No pre-treatment was applied before
160 the first use. In between experiments, the filters were cleaned by soaking, filtering and backflushing for
161 30 min with NaOH 2 wt% (30 °C), followed by 30 min backflushing air at 1.5 bar. The cleaning
162 procedure was then repeated with dH₂O. dH₂O permeability was measured before each experiment.

163 **2.6 Evaluation of fluxes in iMBR configurations**

164 Filtrations were carried out using a peristaltic pump (Masterflex L/S 7518-00), in which the relation
165 between rpm and flow (mL/min) was calibrated with dH₂O at room temperature without being coupled to
166 any filtration device. Critical and limiting fluxes were assessed by the flux stepping method [18]. The
167 setpoint of the pump was increased step-wise from 8-25 mL/min, recording the permeate flow and the
168 transmembrane pressure (TMP) (measured between the peristaltic pump and the filter with a gauge
169 pressure manometer (GM520, Professional Instruments – measuring range ± 350 mbar) as indicated in
170 Figures 3 and 4). For each setpoint, the filtration proceeded until 160 mL of permeate had been removed
171 (target volume exchange in fed-batch as explained in section 3.2.2). Thereafter, the permeate was returned
172 to the bioreactor through the filter in reverse flow. The reverse flow setpoint was the same as the filtration
173 flow for setpoints higher than 16 mL/min. For lower filtration flows, the reverse flow was constant at 16
174 mL/min.

175 This cycle of filtration and backflushing was repeated 5 times for each setpoint. Flow-TMP graphs were
176 constructed using the TMP read at the end of the 5th filtration of each setpoint flow.

177 During these tests, aeration, agitation, temperature and pH were maintained as during cultivation (section
178 2.3). The experiments were performed with dH₂O and cell cultures at different concentrations (1.7 and 16
179 g/L), corresponding to the ones observed at time 0 h and 20 h during the fed-batch with an N/C ratio of 15
180 N_{mmol}/C_{mol} (section 3.1).

181 **2.7 Fed-batch PHA accumulation in iMBRs**

182 PHA accumulation was performed similarly to the description in section 2.3. The key difference was that
183 when butyrate depletion was detected, 160 mL of cell-free liquid were removed through the filtration
184 modules (hollow fibers loop or ceramic filters). Thereafter, 160 mL of fresh feed (at the concentration of
185 the model effluent, section 2.2) were added, keeping the volume constant at 750 mL throughout the 24 h
186 fed-batch (except for sampling and acid/base addition). Feed addition was done through the filter in
187 reverse flow to reduce membrane fouling. The batch started with 850 mL of inoculum from the SBR and
188 thus the first filtration removed slightly more permeate (260 mL) to reach the 750 mL after the first
189 feeding. The initial concentration of VFA after the first feeding was equivalent to the one provided in
190 experiments in section 2.3 (90 C_{mM}).

191 Based on the results presented in section 3.2.2, the filtration flow was set at 16 mL/min for the hollow
192 fiber module (loop configuration). For the ceramic module, the filtration flow was set at 16 mL/min for
193 the first filtration and at 13 mL/min for the subsequent ones. Feed addition occurred at 16 mL/min in
194 reverse flow. In order to avoid accumulation of feed in the inner space of the filters after feed addition,
195 about 7 mL of permeate were returned to the reactor in reverse flow.

196 **2.8 Analytical methods**

197 Samples taken from the bioreactors were centrifuged at 8000 g for 5 min. The supernatant was filtered
198 through 0.45 μm Nylon filters and analysed for VFA and N-NH_3 concentration as described in [19]. The
199 pellet was washed with distilled water and centrifuged again twice before freeze-drying. The PHA content
200 of the biomass pellet was determined by GC chromatography as described in [19], using methyl-3-
201 hydroxybutyrate (99 %, J&K Scientific[®]) and methyl-3-hydroxyvalerate (≥ 98 %, Sigma-Aldrich[®]) as
202 calibration standards [20]. Total biomass concentration was estimated by measurement of the total
203 suspended solids (TSS) in fresh samples, performed according to standard protocols [21] using glass fiber
204 filters of 0.7 μm pore size (Merk Millipore). PHA concentration (g/L) was obtained by multiplying the
205 TSS (g/L) by the PHA content (wt%). Active biomass concentration (cells excluding PHA or X in g/L)
206 were then estimated by subtracting the calculated PHA (g/L) from the TSS (g/L).

207 Water contact angle (θ°) for the membranes used in the diffusion set-up was measured by the sessile drop
208 method [22] in a goniometer (OCA20, Dataphysics Instruments, Germany). For each membrane, the
209 reported values correspond to the average θ° measured in five random locations, recorded immediately after
210 dropping 1 μL of MiliQ[®] water at room temperature onto the membrane. Membrane surface charge was
211 assessed by the zeta potential, measured in a SurPASS electrokinetic analyzer (Anton Parr, Austria) as
212 described in [23].

213 **3 Results**

214 In order to maximise productivity in a MBR configuration, two aspects have to be met. The first is that
215 the culture is able to sustain PHA accumulation and reach high cell densities. This aspect is evaluated in
216 section 3.1. The second aspect is that the MBR configuration is able to operate for the whole PHA
217 accumulation period and meet the requirements of the culture. This is presented in section 3.2.

218 3.1 Effect of the nitrogen/carbon ratio on culture saturation

219 The main advantage of an MBR is the possibility of operating at a constant volume. Extended PHA
220 accumulation batches (maximising the g PHA/g initial biomass) would be desirable to fully exploit this
221 advantage and minimise the volume of the reactor producing inoculum (SBR). However, it is very
222 common that PHA production ceases when cells reach maximum PHA accumulation capacity. This is a
223 result of operation under severe nitrogen limiting conditions, which maximise PHA accumulation and
224 prevent cell growth [1,24]. Recent studies have reported the possibility of extending the PHA
225 accumulation and increase the PHA productivity by supplying limiting rather than starving nutrient
226 conditions, which allow cell growth and PHA accumulation to occur simultaneously [24].

227 In the present study, four nitrogen to carbon (N/C) ratios were tested during fed-batch PHA accumulation.
228 Feed addition occurred whenever butyrate was exhausted, as previous studies on the same culture
229 evidenced that net PHA production drastically reduced during consumption of the remaining VFA
230 (acetate and propionate) [16]. The culture produced a copolymer (poly(3-hydroxybutyrate-co-3-
231 hydroxyvalerate)) referred simply as PHA in the text and figures.

232 The four N/C ratios tested (expressed in terms of $N_{\text{mmol}}/C_{\text{mol}}$) resulted in 4 different scenarios in terms of
233 nitrogen availability (Figure 5 A). In the two lowest ratios (1.8 and 15) all the nitrogen provided was
234 consumed and both cultures were nitrogen limited for the whole batch. However, the degree of limitation
235 was more severe in the first case, which could be considered nitrogen starved. For the N/C ratio of 30, the
236 culture had nitrogen in excess for the first 12 h, but thereafter became nitrogen limited. At an N/C ratio of
237 50, the culture had excess of nitrogen throughout the cultivation.

238 With the N/C ratio in the model effluent ($1.8 N_{\text{mmol}}/C_{\text{mol}}$), substrate consumption and PHA production
239 considerably slowed down after 6 h (Figure 5 B and C). Cell growth was almost negligible (Figure 5 E),
240 what probably led to a saturation of the cells once they had reached its maximum PHA content of about
241 70 % (Figure 5 G).

242 For the other three N/C ratios tested, the culture had a sustained substrate consumption throughout the 24
243 h (Figure 5 B). For all parameters evaluated, these three experiments behaved almost identically for the
244 first 12 hours (Figure 5). At this point, about 8 g of PHA had been produced (Figure 5 C) at a yield of 0.7-
245 0.8 $C_{\text{mol}} \text{PHA}/C_{\text{mol}} \text{S}$ (Figure 5 H). The productivity observed for these three experiments during the first
246 12 h more than doubled the one observed for the N/C ratio of 1.8 (1.0 vs 0.43 g PHA/(L.h)) (Figure 5 D).
247 From 12 h to 24 h, the behaviour of the culture differed slightly according to the nitrogen loading. Higher
248 nitrogen concentrations enabled a higher production of active biomass (Figure 5 E), which translated into
249 a slightly higher substrate consumption (Figure 5 B). For the nitrogen limited case (N/C ratio of 15), this
250 did not have negative effects on the PHA yield or PHA content. At the end of the batch, these parameters
251 presented values of 0.72 $C_{\text{mol}} \text{PHA}/C_{\text{mol}} \text{S}$ and 78 %, respectively, very close to those obtained in nitrogen
252 starving conditions (Figure 5 H and G). On the other hand, for the N/C ratios of 30 and 50, the higher
253 biomass yield resulted in a decrease in the PHA yield and PHA content, especially remarkable for the N/C
254 ratio of 50 (nitrogen excess throughout the batch). The latter presented a PHA yield of 0.45 $C_{\text{mol}} \text{PHA}/C_{\text{mol}}$
255 S and a decrease of the PHA content from 70 % at 12 h to 60 % at 24 h (Figure 5 H and G). This decrease
256 in the PHA content indicated that the growth response had taken over the PHA accumulation of the
257 culture.

258 The N/C ratio of 30 presented only slightly lower values than the N/C ratio of 15 for all parameters. The
259 differences were usually not significant when considering the measurements' standard deviation, but
260 could already indicate that the growth response was starting to take over at this nitrogen loading.
261 Therefore, a N/C ratio of 15 was chosen for further experiments in MBR configurations.

262 In terms of productivity, the values calculated for the whole 24 h batch were considerably lower than
263 obtained during the first 12 h (Figure 5 D). The reason behind that was an important decrease in the
264 specific substrate consumption rate (q_s) with time (Figure 5 F). Hence, even though the productivity could
265 be greatly enhanced by supplying extra nitrogen and allowing cell division to occur, PHA accumulation
266 rates decreased for all the N/C ratios tested. For the N/C ratio of 15, the productivity decreased from 1.00

267 g PHA/(L.h) at 12 h to 0.78 g PHA/(L.h) after 24 h, being this the scenario with the least drop in
268 productivity (Figure 5 D).

269 **3.2 Evaluation of MBR configurations**

270 **3.2.1 Evaluation of the dMBR configuration**

271 For this configuration, microfiltration membranes were used to create a cell-free compartment, from
272 where clarified broth could be withdrawn without removing cells from the bioreactor (Figure 2). The
273 same compartment could be used to supply fresh medium containing VFA, which could diffuse across the
274 membrane to the cell-containing compartment to support PHA accumulation.

275 In order to maximise PHA productivity with this configuration, VFA diffusion across the membrane had
276 to be at least equal to the substrate consumption rate of the culture (r_s). Therefore, VFA diffusion was
277 measured in different membrane materials (PSf and PVDF) and compared to r_s (36.7 C_{mmols} VFA/h in the
278 experiments in section 3.1). This minimum threshold of VFA diffusion was not reached for any of the
279 membranes (Figure 6 A), and thus the configuration would not be able to sustain the PHA accumulation
280 process.

281 For all experiments, the diffusion rate of each of the VFA (butyrate, propionate, acetate and lactate) was
282 proportional to their concentration, suggesting no preferential membrane selectivity. At a similar pore
283 size, the PSf membrane (0.2 μm) presented a much higher diffusion rate than the PVDF membrane (0.15
284 μm) (19 vs. 5 C_{mmols} VFA/h). With the first, the diffusion was comparable to the achieved with the PVDF
285 membrane at 0.45 μm (18 C_{mmols} VFA/h). Hence, PSf resulted in a higher diffusion rate.

286 The hydrophilicity of the materials was measured by contact angle measurements (Figure 6 B), were
287 values below 90° are generally accepted to correspond to hydrophilic surfaces, while hydrophobic for
288 higher values [22]. According to this, PSf was hydrophilic, but PVDF was slightly hydrophobic, with
289 values around 95° and no significant differences between pore sizes ($p = 0.1$).

290 All membranes presented a negative surface charge at the pH of the feed solution (pH 6.4) (Figure 6 C).
291 At this pH, the VFA also have a negative charge. Thus, charge repulsion could have hindered diffusion
292 across the membrane. For the PVDF membranes, the charge was more negative for the 0.15 μm pore
293 membrane compared to the 0.45 μm , which could be a possible explanation for the reduced VFA
294 diffusion obtained at the lower pore size.

295 Based on these results, the higher VFA diffusion rates obtained with PSf compared to PVDF at a similar
296 pore size could be related to the higher hydrophilicity of this membrane combined with the lower negative
297 charge density.

298 **3.2.2 Evaluation of fluxes iMBR configurations**

299 The main limitation of iMBRs is the occurrence of fouling and the consequent reduction of the membrane
300 performance. This phenomenon has led to the definition of two flux concepts: the critical flux and the
301 limiting flux [18]. The critical flux is the one at which irreversible membrane fouling starts to occur.
302 Assuming weak form behaviour, this can be defined as the point at which the relation between the
303 transmembrane pressure (TMP) and flux starts to deviate from linearity, or the point at which the TMP
304 increases at a constant flux [18]. The limiting flux is the highest flux that can be maintained in a given
305 system. Below this flux, fouling might be forming, but it is still possible to maintain the flux by
306 increasing the TMP. Above the limiting flux, the fouling saturates the filtration capacity of the membrane.
307 Here, the discussion is done in terms of flow (instead of flux) for the ease of comparison between setups
308 with different filtration areas.

309 The ultimate objective of the fed-batch cultivation using MBRs was to remove supernatant every time
310 that butyrate was exhausted and replace it with fresh VFA medium. In order to minimise the time that the
311 culture was in absence of butyrate, the filtration time interval had to be as short as possible, but without
312 surpassing the limiting flow, or in the ideal case, the critical flow. The target was to remove 160 mL of
313 supernatant (about 1/5 of the working volume) in 10 min (16 mL/min). By replacing this volume, the
314 initial concentration of substrate after each feeding would be about 90 C_{mM} of VFA, which was found not

315 inhibitory for the culture in previous studies [16]. The two submerged membrane types (hollow fibers and
316 ceramic filters) were tested at flows between 8-25 mL/min, to determine the critical and limiting fluxes.
317 Two cell concentrations were evaluated (1.7 and 16 g/L), corresponding to the cell concentration at the
318 beginning of the fed-batch and after 20 h, respectively (section 3.1).

319 *Hollow fibers*

320 Two types of hollow fiber configurations were tested: a rod configuration and a loop configuration
321 (described in Figure 3). With the rod configuration, the target flow of 16 mL/min (12.3 L/(h.m²)) could
322 not be attained, even with the initial cell concentration of the fed-batch (1.7 g/L) (Figure 7 A). The pump
323 could not maintain flows over 10 mL/min, which was identified as the limiting flow of the system.

324 The loop configuration was much less prone to fouling. The peristaltic pump could always maintain the
325 setpoint flows at the tested range, even with a concentrated cell culture (16 g/L) (Figure 7 B). In other
326 words, the limiting flow was not reached. At the cell concentration of the beginning of the batch (1.7 g/L),
327 the system did not show significant increases in the TMP in consecutive filtrations at the same setpoint
328 flow (Figure 7 D). Moreover, the relation between TMP and flow was linear for the whole range (Figure 7
329 C). Hence, the results did not show signs of having reached a critical flow.

330 With the cell culture of 16 g/L, the critical flow could be identified at 19 mL/min (14.6 L/(h.m²)). At this
331 point, the TMP vs. flow curve started to deviate from linearity (Figure 7 C), and a slight increase in the
332 TMP in consecutive filtrations could be observed (Figure 7 D). Based on these results, operation of the
333 hollow fiber loop module at 16 mL/min (12.3 L/(h.m²)) was considered for the fed-batch PHA
334 accumulation experiments presented in section 3.3.

335 *Ceramic filters*

336 At the initial cell concentration (1.7 g/L), the ceramic filtration module presented a very similar behaviour
337 to the hollow fiber loop. Neither a limiting flow nor a clear critical flow could be identified (Figure 8).
338 The pump could always maintain the setpoint flow (Figure 8 A) and there were no clear deviations from

339 linearity in the curve of TMP vs. flow (Figure 8 B). No significant increase in the TMP was observed in
340 successive filtrations at the same setpoint (Figure 8 C).

341 At the high cell concentration (16 g/L) though, important fouling was observed. Already at 13 mL/min,
342 the TMP increased considerably from the first to the fifth filtration (Figure 8 C), and the TMP increased
343 exponentially in relation to the flow (Figure 8 C). The critical flow was identified at about 13 mL/min
344 (28.2 L/(h.m²)), although lower flows should be tested to better identify the linear region of the curve of
345 TMP vs. flow in Figure 8 B. At 13 mL/min irreversible fouling started to occur, but it was not until much
346 higher flows (25 mL/min) where flow reduction was observed (Figure 8 A) (limiting flow).

347 Given that the system presented clear fouling at the target flow (16 mL/min), an additional anti-fouling
348 strategy was considered, consisting of backflushing air through the filter. This is a common cleaning
349 strategy [6], which can be applied in non-filtration periods for fed-batch processes [25]. The filters
350 presented a very high resistance to air and very little air flow could be obtained at pressures lower than
351 1.5 bar. At this pressure, 250 mL/min of air could be transferred. However, when this strategy was tested
352 with the cell culture, it led to intense foam formation, which could not be controlled even with addition of
353 antifoam at concentrations above the recommended by the supplier (Antifoam 204 Sigma-Aldrich at
354 0.2%). Hence, air backflushing could not be applied as additional antifouling strategy.

355 In order to avoid fouling and eventual saturation of the filters, operation below the critical flux is
356 preferred. For the present case, a sub-critical flux would represent a decrease in the productivity of the
357 system, as it would extend substrate-limiting periods. Based on these results the fed-batch PHA
358 accumulation with ceramic filters operated at 13 mL/min (28.2 L/(h.m²)), which was already at the critical
359 flow, but far below the limiting flow. A flow of 16 mL/min was applied to the first filtration of the batch,
360 as this was below the critical flow observed for the cell concentration at the beginning of the batch.

361 3.3 Fed-batch PHA accumulation in iMBRs

362 Hollow fibers (loop configuration) and ceramic filters were tested in a fed-batch PHA accumulation
363 regime using synthetic VFA medium. The two systems presented very similar results (Figure 9).

364 The filters were used to remove permeate during the fed-batch (1/5 of the working volume) whenever
365 butyrate was consumed. Fresh feed solution was then provided through the filter in reverse flow. During a
366 24 h experiment, this procedure occurred over 20 times, without observing any reduction on the filtration
367 flow (Figure 9 A and D). Both iMBRs allowed to feed over 3.5 L of substrate through the reactor, while
368 keeping the working volume at 0.75 L. As a result, they enabled an 82 % reduction on the working
369 volume, compared to a scenario where these experiments would be performed without a cell-retention
370 system. The concentration of PHA at this point was 18.5 g/L (Figure 9 B and E).

371 The use of submerged filtration during PHA accumulation resulted in high values of productivity (0.87-
372 1.44 g PHA/(L.h)) (Figure 9 C and F). However, a decrease of PHA productivity was observed during the
373 fed-batch, especially after 12 h, as already observed in the experiments without cell-retention systems
374 presented in section 3.1. After 12 h, the productivity was 1.20 and 1.27 g PHA/(L.h), for hollow fibers
375 and ceramic filters, respectively. At 24 h, the values decreased to 0.89 and 0.87 g PHA/(L.h),
376 respectively. If stopped after 12 h, the bioreactors would present a total TSS concentration of about 20
377 g/L with a PHA content of 70 % PHA (14 g PHA/L) (Figure 9 B and D). At this point, the use of iMBRs
378 would represent a 75 % reduction of the working volume with respect to a system without cell recycling
379 (about 2 L of feed had been circulated).

380 Overall, despite the iMBRs were capable of sustainable operation for 24 h, such long cultivations would
381 not appear as a clear choice looking exclusively at the values of productivity during PHA accumulation
382 (Figure 9 C and F). However, the perspective might change when taking into consideration the volume
383 and duration of the cycle of the SBR (innoculum reactor), and the overall productivity of the process; as
384 extended PHA accumulation batches would bring a reduction of the inoculum need and thus a reduction
385 of the SBR reactor.

386 It is important to mention that the results presented for the hollow fibers module were obtained with a
387 periodical rotation of the hollow fiber module during the fed-batch to release the cell cake. When this
388 procedure was not done, considerable cell deposition was observed on the hollow fibers, and in the zones
389 in contact with the wall of the reactor. The cake did not affect the performance of the membrane, which
390 could still maintain the flow during the whole 24 h fed-batch, but it compromised the performance of the
391 culture and the determination of microbial biomass. By slightly rotating the filter, cell deposits were
392 released by the turbulence created by the agitation and aeration. Immediately after rotating, the
393 concentration of suspended cells would increase by 13 %, and a drop in the oxygen saturation was
394 observed, indicating an increase in the metabolism. It is a known fact that oxygen and substrate can
395 become limiting in the inner layers of the cake, in which the cells are at risk of death [26]. In the present
396 setup, cake formation led to a decrease of 46 % in the substrate consumed and PHA produced (when
397 considering the whole 24 h batch). Such an important effect could be a result of the limited space between
398 the fiber loop and the wall of the reactor (Figure 3 B), which allowed little movement of the fibers.

399 **4 Discussion**

400 **4.1 Perspectives on the use of dMBRs for PHA production**

401 With the reactor design and membranes studied in this work, diffusion of VFA across the membrane did
402 not meet the substrate requirements of the culture (section 3.2.1). At the highest porosity tested, PSf (0.2
403 μm) and PVDF (0.45 μm) allowed for a diffusion rate between 18-19 C_{mmol} VFA/h (corresponding to a
404 flux of 576-610 $C_{\text{mmol}}/(\text{h}\cdot\text{m}^2)$) (Figure 6). This value should have been double in order to meet the
405 substrate requirements of the present culture (36 C_{mmol} VFA/h).

406 Diffusion rate of VFA across the membranes is proportional to the membrane surface and the
407 concentration difference between the two sides of the membrane [15]. Thus, the strategy could still be
408 valuable in a reactor design with double surface of contact. In the same line, substrate requirements could
409 be met with a feed solution of approximately double VFA concentration (assuming a proportional

410 concentration polarisation effect). This would correspond to a concentration of about 20 g/L of VFA,
411 which is common in many fermentation effluents [5]. However, even in that scenario, the concentration of
412 VFA in the feed side would decrease as acids diffuse to the cell compartment, decreasing the
413 transmembrane gradient. Hence, the VFA diffusion rate would decrease with time, eventually leading
414 again to a situation where substrate requirements would not be met. A possible way to achieve a constant
415 VFA flux would be a continuous recirculation of broth from the fermentation bioreactor to the feed
416 compartment of the PHA accumulating reactor, similar to what was suggested by Du and Yu [27].
417 In regards to membrane materials, the results showed higher diffusion rates with PSf compared to PVDF,
418 with the first being more hydrophilic. Higher diffusion for hydrophilic materials was also reported by Du
419 and Yu [27] and Youngsukkasem et al. [28], which are, to our knowledge, the only previous reports
420 evaluating VFA diffusion studies in a similar context. Moreover, the present study showed that VFA
421 diffusion was highly correlated with the negative charge density on the membrane surface (Figure 6),
422 possibly justified by repulsive forces with the ionised carboxyl groups of VFA at pH 6.4. To reverse these
423 interactions, the pH should be lower than the isoelectric point of the membranes (about pH 4 in Figure 6
424 C), or lower than the pKa of the acids (3.8 – 4.9). Given that these are rather low values of pH to carry out
425 a biological process, it would be interesting to study other hydrophilic membrane materials with positive
426 or neutral surface charge at a higher pH range.

427 Small pore sizes are generally preferred in iMBR applications, as they minimise pore clogging by
428 microbial cells [26]. Yet, our results showed that smaller pore size had an important effect on the charge
429 density and led to lower diffusion rates. Therefore, bigger pore sizes might be beneficial for diffusion-
430 based applications.

431 **4.2 Perspectives on the use of iMBRs for PHA production**

432 This section discusses the main challenges and opportunities identified with the use of iMBR
433 configurations (hollow fibers and ceramic filters) for PHA production, summarised in Table 1.

434 Two types of hollow fiber configurations were tested in this study: a rod configuration and a loop
 435 configuration (Figure 3). As described in section 3.2.2, the rod configuration was more prone to fouling
 436 than the loop. In the rod, the fibers were very compact, allowing little circulation of liquid in between.
 437 Conversely, the loop configuration allowed for a more free movement of air and liquid in between the
 438 fibers, which provided membrane scouring and alleviated fouling. However, this looser configuration also
 439 led to higher fiber surface, creating a cell-retention net. Cells would get trapped in this fiber net, and
 440 between the fibers and the reactor wall, resulting in cell deposits. As explained in section 3.3, this did not
 441 lead to problems of membrane operation, but it led to an important decrease on the substrate consumption
 442 rate (46 %), most likely caused by substrate and oxygen limitation in the inner layers of the cell cake. In
 443 the current setup, this could be solved by rotating the fibers, what changed the flow patterns between the
 444 fibers and released the cell cake. This aspect would be of critical relevance when considering a scale-up
 445 of the process, especially considering that the product (PHA) would also be trapped.

446 Table 1: Main opportunities and challenges of hollow fibers (loop configuration) and ceramic filters
 447 applied as submerged filtration systems during PHA accumulation.

| | Hollow fibers | Ceramic filters |
|---------------------------|---|---|
| Advantages /opportunities | <ul style="list-style-type: none"> Stable permeate flux during 24 h fed-batch process. Low relation footprint/filtration area. | <ul style="list-style-type: none"> Stable permeate flux during 24 h fed-batch process. Not prone to cell cake formation. More resistant to chemical cleaning. Possibility to couple to PHA purification through chemical digestion methods.* |
| Disadvantages /challenges | <ul style="list-style-type: none"> Prone to cake formation. The fiber net traps cells leading to reduced cell activity and lower PHA production. | <ul style="list-style-type: none"> High relation footprint/filtration area. |

*According to literature information. Not tested in this study.

448

449 Cake formation was not an issue in ceramic filters. Their tubular smooth surface was not prone to
450 accumulate cells under the turbulent flow pattern in the bioreactor. However, the ceramic filters presented
451 a lower critical flow compared to the hollow fiber loop (13 vs. 19 mL/min) (section 3.2.2). This was a
452 result of the three times bigger filtration surface provided by the hollow fibers (779 cm² vs. 276 cm²). In
453 terms of flux, the critical point was higher for the ceramic filters (28.2 vs. 14.6 L/(h.m<sup>2454 limitations in the bioreactor impeded the possibility of increasing the surface of filtration. Given the lesser
455 propensity of ceramic filters to cell cake formation, it would be interesting to explore filter configurations
456 that could increase the filtration area without increasing the footprint.</sup>

457 A successful fed-batch operation with effluent removal and no flow reduction could be attained with both
458 the hollow fiber loop and the ceramic filters (section 3.3). Both systems operated below their limiting
459 flow allowed a rapid exchange of exhausted supernatant for fresh medium (aprox. 10 min). However, to
460 minimise periods without substrate, the ceramic module was operated above its critical flow towards the
461 end of the batch, when high cell concentrations were reached (according to the results in Figure 8 section
462 3.2.2). At this point of the discussion, it is interesting to introduce the concept of the sustainable flux [18].
463 Operation below the critical flux, where no fouling occurs, is a good strategy to prolong membrane
464 performance and to minimise the costs of membrane cleaning. However, operation at such fluxes might
465 not be feasible for certain processes. Instead, it might be feasible to operate at fluxes with a low fouling
466 rate, in which the cost and downtime from membrane cleaning are reasonable. In this respect, it would be
467 interesting to consider the integration of membrane cleaning and PHA recovery. In recent years, PHA
468 recovery methods based on the use of chemicals to digest and solubilise non-PHA material have gained
469 interest. Such processes involve the same type of chemicals used for membrane cleaning (alkalis, acids or
470 oxidizing agents) [1,6,20], and thus integration of both operations could be envisioned. In this regard,
471 ceramic membranes would offer an additional advantage, given their higher resistance to chemicals and
472 overall robustness [7].

473 The main objective of this study was not to define a sustainable flux, which should be studied in real
474 effluents and considering a long-term performance of the systems, but to perform a proof of concept of
475 the utilisation of MBRs for PHA accumulation. In this sense, both iMBR configurations proved valuable
476 to overcome the limitations of dilute feeding solutions, reaching high PHA productivities (0.87-1.44 g
477 PHA/(L.h)). These values are among the highest reported for PHA production processes in MMC -
478 generally below 0.5 g/(L.h) [5] - showing the great potential of this cultivation strategy. Besides being
479 valuable for fed-batch cultivations, iMBR could also be an asset in PHA production in continuous mode,
480 as they could offer the possibility of uncoupling the hydraulic retention time from the cell retention time
481 and cell growth.

482

483 **5 Conclusions**

484 One of the main limitations to obtain high PHA productivities with second-generation substrates is the
485 dilute nature of the feed solutions. The present study evaluated for the first time the use of membrane
486 bioreactors (MBRs) in the frame of PHA production in mixed microbial consortia. The main conclusions
487 of the work were:

- 488 • In pressure-driven immersed MBR configurations (iMBR), both hollow fibers and ceramic filters
489 allowed to feed over 3.5 L of substrate in a fed-batch period of 24 h, while keeping a constant
490 reactor volume of 0.75 L, representing an 82 % reduction of the reactor volume.
- 491 • A high volumetric productivity could be attained in iMBR configurations (0.87-1.44 g
492 PHA/(L.h)) despite the use of a diluted substrate feed (approximately 10 g/L of volatile fatty
493 acids).
- 494 • Hollow fibers allowed to operate at higher flows, due to their lower ratio of surface/footprint.
495 However, they presented a risk of cell deposition, resulting in a decreased metabolic activity and
496 PHA production rate.

- 497 • Ceramic filters were less prone to cell deposition and fouling, but they had a higher footprint,
498 leading to a lower critical flow with the surface available in the bioreactor.
- 499 • VFA diffusion across PSf and PDVF microfiltration membranes was not enough to satisfy the
500 substrate requirements of the culture in a novel diffusion-based MBR configuration.

501 **Acknowledgements**

502 This work was financed by the Technical University of Denmark. The authors thank Mingbo Ji for the
503 contact angle and the zeta potential measurements.

504 **References**

- 505 [1] C. Kourmentza, J. Plácido, N. Venetsaneas, A. Burniol-Figols, C. Varrone, H.N. Gavala,
506 M.A.M. Reis, Recent Advances and Challenges towards Sustainable
507 Polyhydroxyalkanoate (PHA) Production, *Bioengineering*. 4 (2017) 1–43.
508 <https://doi.org/10.3390/bioengineering4020055>.
- 509 [2] W. Blunt, D.B. Levin, N. Cicek, Bioreactor Operating Strategies for Improved
510 Polyhydroxyalkanoate (PHA) Productivity, *Polymers (Basel)*. 10 (2018) 1197.
511 <https://doi.org/10.3390/polym10111197>.
- 512 [3] J.L. Ienczak, W. Schmidell, G.M.F. De Aragão, High-cell-density culture strategies for
513 polyhydroxyalkanoate production: A review, *J. Ind. Microbiol. Biotechnol.* 40 (2013)
514 275–286. <https://doi.org/10.1007/s10295-013-1236-z>.
- 515 [4] M. Koller, L. Maršálek, M.M. de Sousa Dias, G. Braunegg, Producing microbial
516 polyhydroxyalkanoate (PHA) biopolyesters in a sustainable manner, *N. Biotechnol.* 37
517 (2017) 24–38. <https://doi.org/10.1016/j.nbt.2016.05.001>.

- 518 [5] F. Valentino, F. Morgan-Sagastume, S. Campanari, M. Villano, A. Werker, M. Majone,
519 Carbon recovery from wastewater through bioconversion into biodegradable polymers, N.
520 Biotechnol. 37 (2016) 9–23. <https://doi.org/10.1016/j.nbt.2016.05.007>.
- 521 [6] S. Judd, The MBR book: principles and applications of membrane bioreactors for water
522 and wastewater treatment., Second edi, Elsevier, 2010. ISBN: 9780080966823.
- 523 [7] F. Carstensen, A. Apel, M. Wessling, In situ product recovery: Submerged membranes vs.
524 external loop membranes, J. Memb. Sci. 394–395 (2012) 1–36.
525 <https://doi.org/10.1016/j.memsci.2011.11.029>.
- 526 [8] W.S. Ahn, S.J. Park, S.Y. Lee, Production of poly(3-hydroxybutyrate) from whey by cell
527 recycle fed-batch culture of recombinant *Escherichia coli* , Biotechnol. Lett. 23 (2001)
528 235–240. <https://doi.org/10.1023/A:1005633418161>.
- 529 [9] C. Haas, T. El-najjar, N. Virgolini, M. Smerilli, M. Neureiter, High cell-density
530 production of poly(3-hydroxybutyrate) in a membrane bioreactor, N. Biotechnol. 37
531 (2017) 117–122. <https://doi.org/10.1016/j.nbt.2016.06.1461>.
- 532 [10] J.L. Ienczak, M. Schmidt, L.K. Quines, Poly(3-Hydroxybutyrate) Production in Repeated
533 fed-Batch with Cell Recycle Using a Medium with low Carbon Source Concentration,
534 Appl. Biochem. Biotechnol. 178 (2016) 408–417. <https://doi.org/10.1007/s12010-015-1883-9>.
- 535
- 536 [11] M. Schmidt, J. Lutz, L. Kelin, K. Zanonato, W. Schmidell, G. Maria, F. De Aragão,
537 Poly(3-hydroxybutyrate-co-3-hydroxyvalerate) production in a system with external cell
538 recycle and limited nitrogen feeding during the production phase, Biochem. Eng. J. 112
539 (2016) 130–135. <https://doi.org/10.1016/j.bej.2016.04.013>.

- 540 [12] M. Gander, B. Jefferson, S. Judd, Aerobic MBRs for domestic wastewater treatment: A
541 review with cost considerations, *Sep. Purif. Technol.* 18 (2000) 119–130.
542 [https://doi.org/10.1016/S1383-5866\(99\)00056-8](https://doi.org/10.1016/S1383-5866(99)00056-8).
- 543 [13] L.H. de Andrade, F.D. dos S. Mendes, J.C. Espindola, M. Amaral, Internal versus external
544 submerged membrane bioreactor configurations for dairy wastewater treatment, *Desalin.*
545 *Water Treat.* 52 (2014) 16–18. <https://doi.org/10.1080/19443994.2013.799048>.
- 546 [14] P. Kumar, H. Jun, B. Soo, Co-production of polyhydroxyalkanoates and carotenoids
547 through bioconversion of glycerol by *Paracoccus* sp. strain LL1, *Int. J. Biol. Macromol.*
548 107 (2018) 2552–2558. <https://doi.org/10.1016/j.ijbiomac.2017.10.147>.
- 549 [15] A. Mahboubi, P. Ylittervo, W. Doyen, H. De Wever, M.J. Taherzadeh, Reverse membrane
550 bioreactor: Introduction to a new technology for biofuel production, *Biotechnol. Adv.* 34
551 (2016) 954–975. <https://doi.org/10.1016/j.biotechadv.2016.05.009>.
- 552 [16] A. Burniol-Figols, C. Varrone, S.B. Le, A.E. Daugaard, I. V. Skiadas, H.N. Gavala,
553 Combined polyhydroxyalkanoates (PHA) and 1,3-propanediol production from crude
554 glycerol: Selective conversion of volatile fatty acids into PHA by mixed microbial
555 consortia, *Water Res.* 136 (2018) 180–191. <https://doi.org/10.1016/j.watres.2018.02.029>.
- 556 [17] C. Varrone, I. V. Skiadas, H.N. Gavala, Effect of hydraulic retention time on the
557 modelling and optimization of joint 1,3 PDO and BuA production from 2G glycerol in a
558 chemostat process, *Chem. Eng. J.* 347 (2018) 525–534.
559 <https://doi.org/10.1016/j.cej.2018.04.071>.
- 560 [18] P. Bacchin, P. Aimar, R.W. Field, Critical and sustainable fluxes: Theory, experiments
561 and applications, *J. Memb. Sci.* 281 (2006) 42–69.

- 562 <https://doi.org/10.1016/j.memsci.2006.04.014>.
- 563 [19] A. Burniol-Figols, C. Varrone, A.E. Daugaard, S.B. Le, I. V. Skiadas, H.N. Gavala,
564 Polyhydroxyalkanoates (PHA) production from fermented crude glycerol: Study on the
565 conversion of 1,3-propanediol to PHA in mixed microbial consortia, *Water Res.* 128
566 (2018) 255–266. <https://doi.org/10.1016/j.watres.2017.10.046>.
- 567 [20] A. Burniol-Figols, I. V. Skiadas, A.E. Daugaard, H.N. Gavala, Polyhydroxyalkanoate
568 (PHA) purification through dilute aqueous ammonia digestion at elevated temperatures, *J.*
569 *Chem. Technol. Biotechnol.* 95 (2020) 1519-1532.
570 <https://doi.org/https://doi.org/10.1002/jctb.6345>.
- 571 [21] APHA, AWWA, WEF, Standard Methods for the Examination of Water & Wastewater,
572 21st editi, American Public Health Association (APHA), Washington, DC, USA, 2005.
573 ISBN: 0875530478.
- 574 [22] R.S. Hebbar, A.M. Isloor, A.F. Ismail, Contact Angle Measurements, in: N. Hilal, A.F.
575 Ismail, T. Matsuura, D. Oatley-Radcliffe (Eds.), *Membr. Charact.*, Elsevier B.V., 2017.
576 ISBN: 9780444637765: pp. 219–255. [https://doi.org/10.1016/B978-0-444-63776-](https://doi.org/10.1016/B978-0-444-63776-5.00012-7)
577 [5.00012-7](https://doi.org/10.1016/B978-0-444-63776-5.00012-7).
- 578 [23] Y. Zhang, J. Wang, F. Gao, Y. Chen, H. Zhang, A comparison study: The different
579 impacts of sodium hypochlorite on PVDF and PSF ultrafiltration (UF) membranes, *Water*
580 *Res.* 109 (2017) 227–236. <https://doi.org/10.1016/j.watres.2016.11.022>.
- 581 [24] F. Valentino, L. Karabegovic, M. Majone, F. Morgan-Sagastume, A. Werker,
582 Polyhydroxyalkanoate (PHA) storage within a mixed-culture biomass with simultaneous
583 growth as a function of accumulation substrate nitrogen and phosphorus levels, *Water*

- 584 Res. 77 (2015) 49–63. <https://doi.org/10.1016/j.watres.2015.03.016>.
- 585 [25] T. Suzuki, A Dense Cell Retention Culture System Using a Stirred Ceramic Membrane
586 Reactor, *Biotechnol. Bioeng.* 44 (1994) 1186–1192.
587 <https://doi.org/10.1002/bit.260441005>.
- 588 [26] O.T. Iorhemen, R.A. Hamza, J.H. Tay, Membrane Bioreactor (MBR) Technology for
589 Wastewater Treatment and Reclamation : Membrane Fouling, *Membranes.* 6 (2016) 1–29.
590 <https://doi.org/10.3390/membranes6020033>.
- 591 [27] G. Du, J. Yu, Green Technology for Conversion of Food Scraps to Biodegradable
592 Thermoplastic Polyhydroxyalkanoates, 36 (2002) 5511–5516.
593 <https://doi.org/10.1021/es011110o>.
- 594 [28] S. Youngsukkasem, H. Barghi, S.K. Rakshit, M.J. Taherzadeh, Rapid Biogas Production
595 by Compact Multi-Layer Membrane Bioreactor: Efficiency of Synthetic Polymeric
596 Membranes, *Energies.* 6 (2013) 6211–6224. <https://doi.org/10.3390/en6126211>.
- 597

Figures

Figure 1: Schematic representation of different membrane bioreactor (MBR) configurations.

Alternative reactor designs are possible for each configuration. Modified from [15].

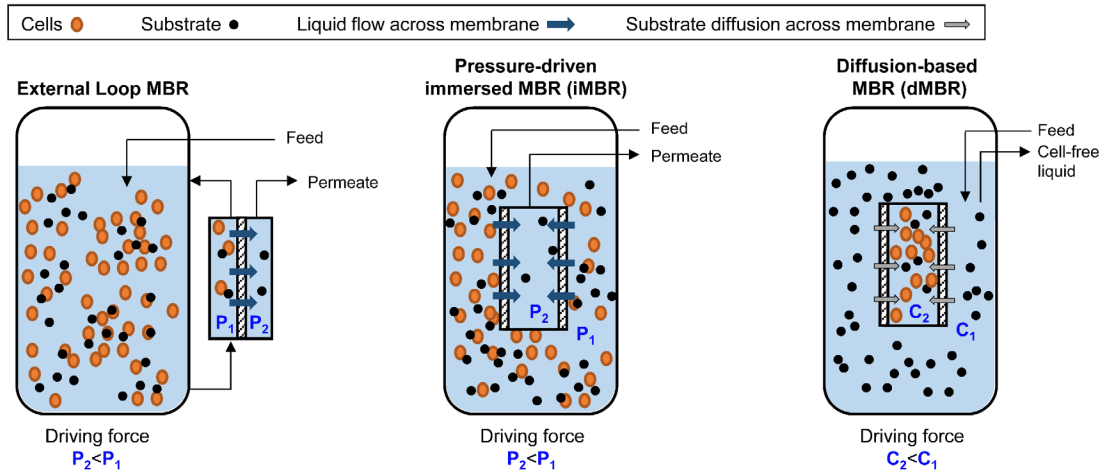


Figure 2: Diffusion-based membrane bioreactor (dMBR). A: Membrane support. B: Schematic representation of the diffusion membrane inside the bioreactor. Blue arrows indicate diffusion across the membrane.

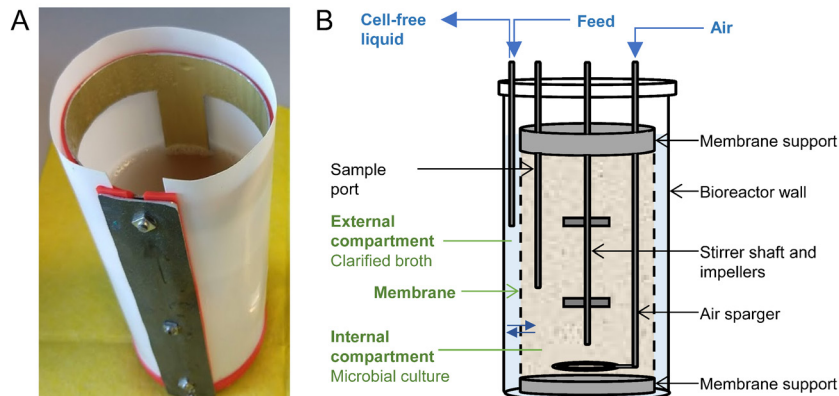


Figure 3: Hollow fiber configurations. A: Rod configuration. B: Loop configuration placement in the bioreactor. C: Schematic representation of the hollow fiber rod module inside the bioreactor.

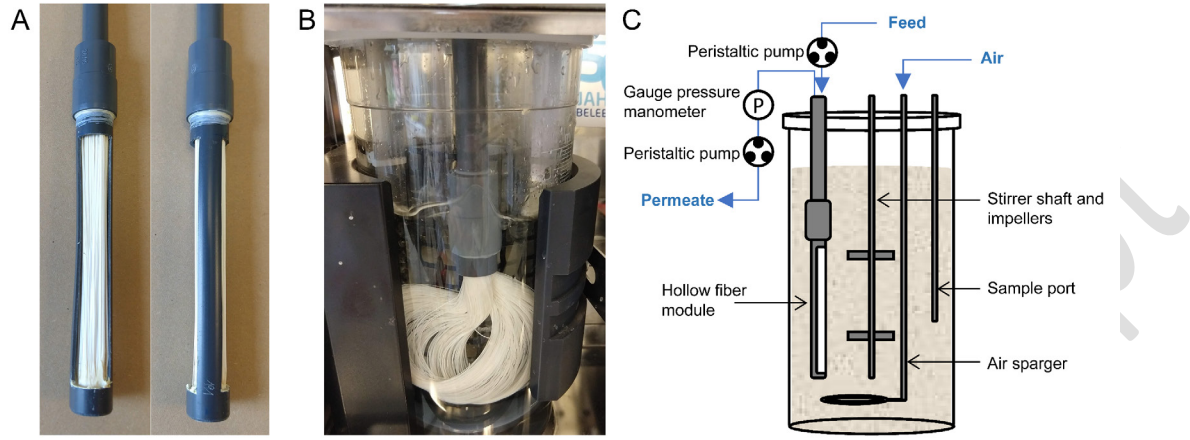


Figure 4: A: Ceramic filtration module. B: Schematic representation of the ceramic filtration module inside the bioreactor

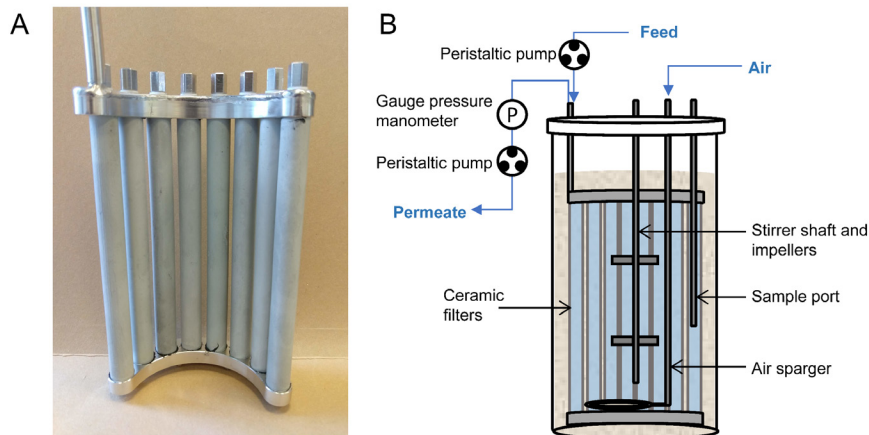


Figure 5: Fed-batch PHA accumulation experiments at different nitrogen/carbon ratios. *In order to better reflect the obtainable productivity in a membrane bioreactor configuration with constant volume, volumetric productivity was calculated considering a constant volume equal to the initial volume.

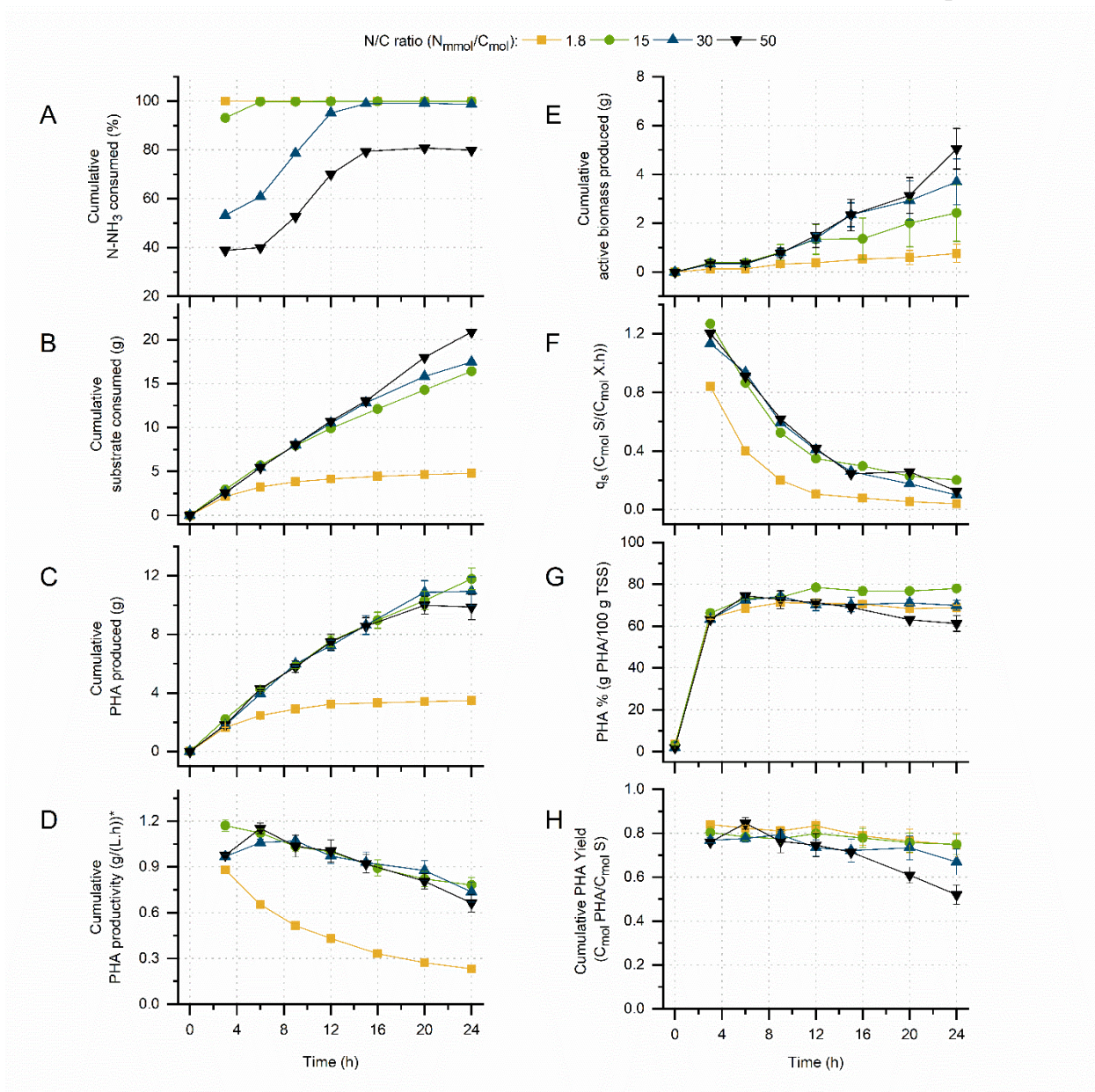


Figure 6: Results of the diffusion-based MBR with PSf and PVDF membranes at different pore size. A:VFA diffusion across the membranes ($C_{\text{mmols/h}}$). The dashed line across the graph indicates the substrate consumption rate of the culture (r_s) ($C_{\text{mmols/h}}$). B: Water contact angle. C: Zeta Potential.

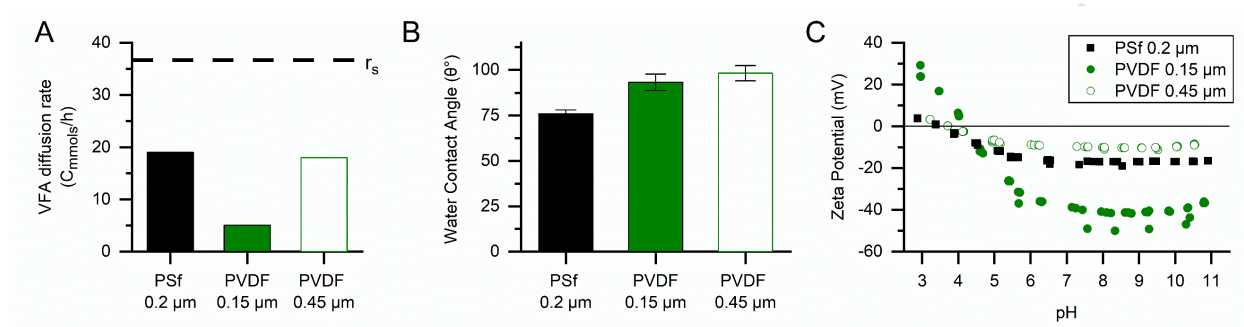


Figure 7: Evaluation of critical and limiting flux for the hollow fiber modules. A: Rod configuration. B, C and D: Loop configuration. In graphs A, B and C, the values of flow and transmembrane pressure (TMP) are the ones recorded at the end of the 5th filtration at each flow setpoint.

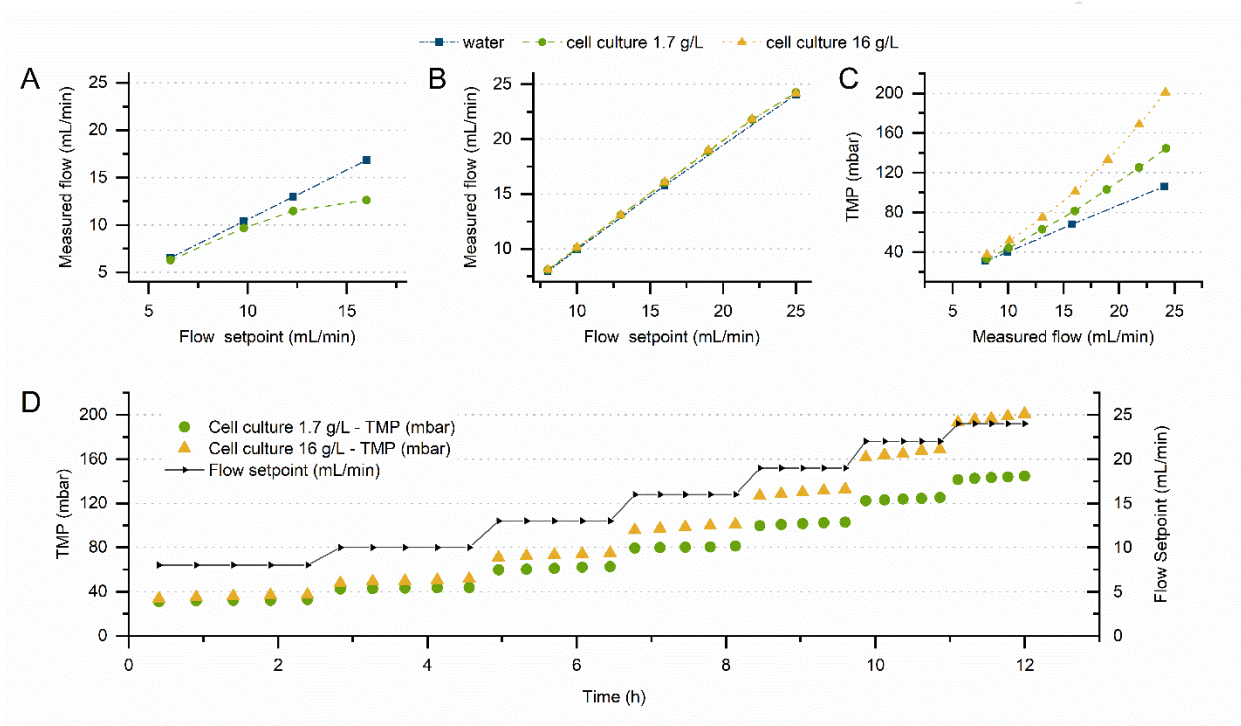


Figure 8: Evaluation of critical and limiting flux for the ceramic filtration module. In graphs A and B, the values of flow and transmembrane pressure (TMP) are the ones recorded at the end of the 5th filtration at each flow setpoint.

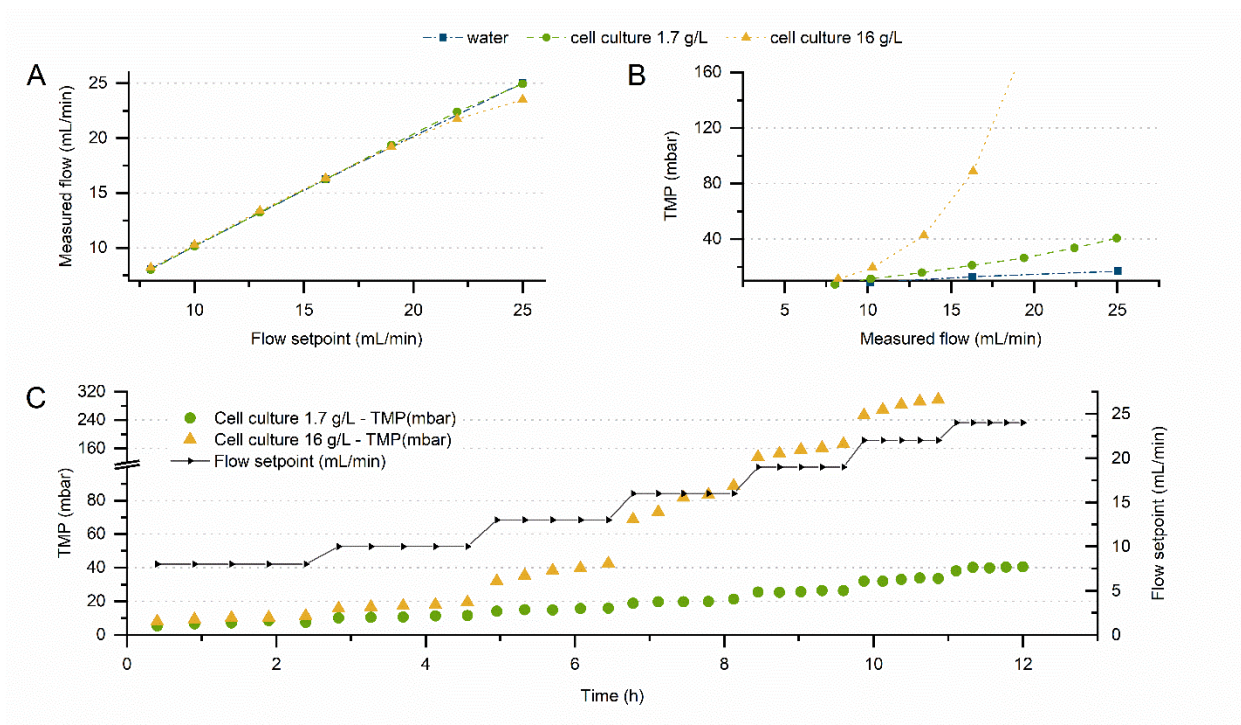


Figure 9: Fed-batch PHA accumulation in iMBR (pressure-driven immersed bioreactors): loop hollow fibers (left) and ceramic filters (right).

